

## Doubly resonant Raman scattering in the semimagnetic semiconductor $\text{Cd}_{0.95}\text{Mn}_{0.05}\text{Te}$

S. I. Gubarev,\* T. Ruf, and M. Cardona

*Max-Planck-Institut für Festkörperforschung, Heisenbergstrasse 1,  
D-7000 Stuttgart 80, Germany*

(Received 18 July 1990)

Doubly resonant Raman scattering (DRRS) has been observed for first-order LO-phonon scattering in the semimagnetic semiconductor  $\text{Cd}_{0.95}\text{Mn}_{0.05}\text{Te}$  (001). The DRRS conditions were realized by tuning the magnetic field, which produces a giant spin splitting of the exciton states due to the strong exchange interaction with the magnetic ions of the crystal. The double resonance was observed with crossed polarizations in the  $z(\sigma^+, \sigma^-)\bar{z}$  configuration and reveals a very narrow profile with a half-width  $\Gamma=2.3$  meV. The analysis of selection rules and excitation energies for double resonance shows that DRRS is connected with the electron transitions from  $|\frac{3}{2}, -\frac{3}{2}\rangle$  to the  $|\frac{3}{2}, \frac{1}{2}\rangle$  valence states split by exchange interaction.

### INTRODUCTION

Doubly resonant first-order Raman scattering (DRRS) occurs when simultaneous resonance of the incident and scattered light with electronic interband transitions is achieved in the crystal. Under these conditions, both denominators involved in the expression for the Raman process resonate at the same time, a fact that leads to a drastic enhancement of the Raman scattering efficiency. DRRS has been experimentally observed in bulk GaAs (Refs. 1 and 2) and in GaAs- $\text{Al}_{1-x}\text{Ga}_x\text{As}$  quantum-well structures.<sup>3,4</sup> In order to realize the DRRS conditions, the energies of the electronic states of the crystal have to be adjusted so that the difference between two interband transitions is equal to the phonon energy. In quantum-well structures (QWS), the DRRS condition has been achieved by a proper choice of the QWS parameters<sup>3</sup> or by applying an electric field perpendicular to the QWS.<sup>4</sup> In bulk materials such an adjustment has been carried out by means of the uniaxial stress, which splits the valence-band states,<sup>1</sup> or by applying a magnetic field and tuning the Landau-level energies to the DRRS condition.<sup>2</sup>

Semimagnetic semiconductors (SMS) offer new possibilities of achieving DRRS. The strong exchange interaction typical of these materials leads to a large spin splitting of the exciton states in the magnetic field.<sup>5</sup> The value of this splitting can reach  $\sim 100$  meV, which exceeds typical LO-phonon energies in SMS. The dependence of the exchange field (and consequently the exciton spin splitting) on temperature and magnetic field makes it possible to change the exciton energies and spin splittings so as to meet the DRRS condition. An enhancement of the LO-phonon Raman scattering near the resonance condition has been reported in Ref. 6. The resonance behavior of the efficiency for Raman scattering by one LO phonon under spin splitting of the exciton state in  $\text{Cd}_{1-x}\text{Mn}_x\text{Te}$  has been studied in Ref. 7, but no features related to double resonance were reported.

In this paper, the resonance behavior of Raman

scattering in  $\text{Cd}_{1-x}\text{Mn}_x\text{Te}$  ( $x=0.05$ ) has been investigated around double-resonance conditions when the energies of incident and scattered light coincide with real exciton states split by the exchange interaction with magnetic impurities.

### EXPERIMENT

$\text{Cd}_{1-x}\text{Mn}_x\text{Te}$  crystals were grown by a modified Bridgman method with a nominal Mn concentration of  $x \approx 0.05$ . This value is in good agreement with  $x=0.052$  obtained from the energy position of the exciton line measured from reflectivity data.<sup>8</sup> Samples were mounted in an optical exchange gas cryostat with the sample temperature about 5 K. A superconducting solenoid giving fields up to 12.8 T was used. The measurements were performed in the backscattering Faraday geometry with the direction of incident and scattered light perpendicular to the (001) crystal surface. A tunable Ti sapphire laser pumped with an  $\text{Ar}^+$ -ion laser was used as a light source. The double monochromator SPEX 1404 was set at the scattered frequency and operated as a spectral bandpass with the width of 0.2 meV. A cooled GaAs photomultiplier and conventional photon-counting electronics were used to measure the scattering efficiency. For each excitation energy, this efficiency was determined as a function of the magnetic field (magneto-Raman profile) for different circular polarizations of the exciting and scattered light. Because the exciton spin splitting is very sensitive to temperature, the laser power was attenuated to 1 mW to prevent sample heating.

### EXPERIMENTAL RESULTS

Exchange interaction with a magnetic impurity leads to a strong spin splitting of the exciton states in the magnetic field. Figure 1 shows exciton energies obtained from reflectivity data as a function of magnetic field. Four exciton transitions are optically active in the Faraday configuration, two in the  $\sigma^+$  and two in the  $\sigma^-$  polarizations. The total splitting between the exciton com-

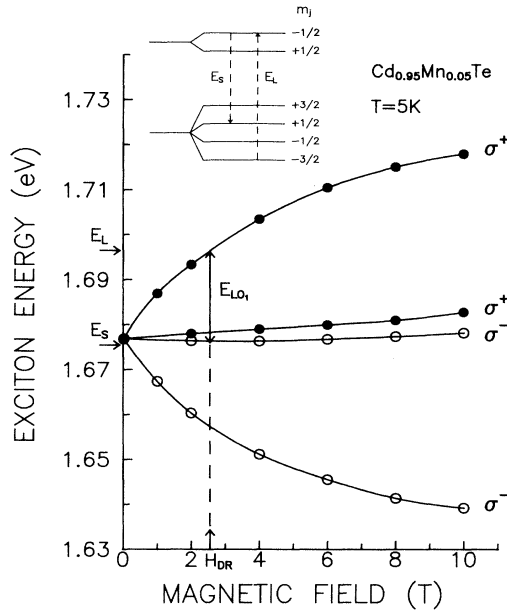


FIG. 1. Exciton energies vs magnetic field  $H$  obtained from reflectivity data in  $\sigma^+$  (●) and  $\sigma^-$  (○) polarizations. Arrows show the DRRS conditions realized experimentally in  $z(\sigma^+, \sigma^-)\bar{z}$  configuration. The scheme of interband optical transitions involved in the DRRS is shown in the inset. The lines are a guide to the eye.

ponents in the magnetic field  $H=10$  T is equal to 80 meV. The arrows in Fig. 1 show the DRRS condition realized in our study. DRRS occurs at the field  $H_{DR}$  when both the laser energy  $E_L$  and the scattered photon energy  $E_S = E_L - \hbar\Omega_{LO}$  coincide with energies of split exciton states in the crystal.

$\text{Cd}_{1-x}\text{Mn}_x\text{Te}$  is a mixed crystal. The optical phonons of this alloy exhibit the so-called “two-mode” behavior.<sup>6</sup> The Raman spectrum of the investigated  $\text{Cd}_{1-x}\text{Mn}_x\text{Te}$

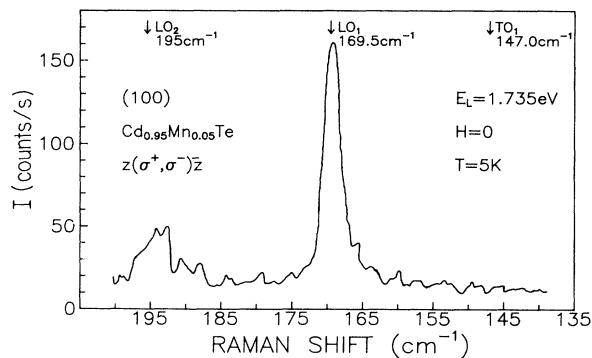


FIG. 2. Spectrum of the first-order Raman scattering measured at  $H=0$  and excitation energy  $E_L=1.735$  eV. The arrows show the positions of the  $\text{LO}_1$ ,  $\text{LO}_2$ , and  $\text{TO}_1$  (forbidden) phonons.

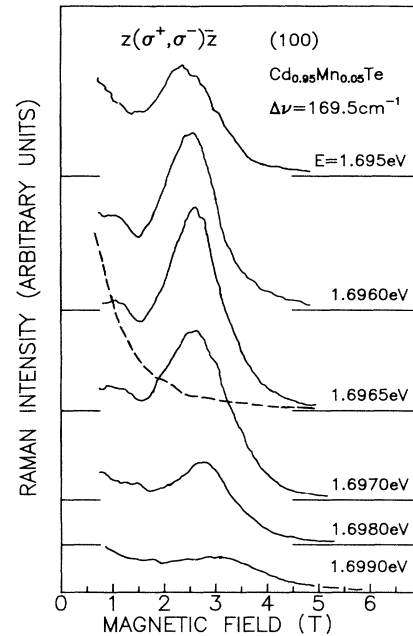


FIG. 3. Raman scattering intensity vs magnetic field  $H$  for different excitation energies  $E_L$  in  $z(\sigma^+, \sigma^-)\bar{z}$  configuration (solid lines). The DRRS scattering conditions correspond to the excitation energy  $E_L=1.6965$  eV. For this case the non-resonant profile [ $z(\sigma^+, \sigma^+)\bar{z}$ ] is also given (dashed line).

crystal is presented in Fig. 2. Two lines with phonon energies  $E_{\text{LO}_1}=169.5$   $\text{cm}^{-1}$  and  $E_{\text{LO}_2}=195$   $\text{cm}^{-1}$  are observed in the RS under excitation above the energy gap. In accordance with Ref. 6 these lines are related to “CdTe-like” and “MnTe-like” LO phonons, respectively. The  $\text{TO}_1$  mode is observed only for excitation in the transparent region, below the lowest exciton energy. No  $\text{TO}_1$  line has been observed for excitation above that energy.

In our experiments, we mainly studied the resonance behavior of the  $\text{LO}_1$  line, which dominates the Raman spectra. Figure 3 shows magneto-Raman profiles of the  $\text{LO}_1$  mode in the vicinity of the DRRS measured for various excitation energies. For the  $z(\sigma^+, \sigma^-)\bar{z}$  configuration, these spectra display a clear maximum at magnetic fields around 2.5 T. The amplitude of the maximum in the resonance profiles depends strongly on the excitation energy and the largest value is found at  $E_L=1.6965$  eV. Hardly any trace of the resonance is seen in the  $z(\sigma^+, \sigma^+)\bar{z}$  configuration (dashed line in Fig. 3). The  $z(\sigma^+, \sigma^-)\bar{z}$  and  $z(\sigma^+, \sigma^+)\bar{z}$  geometries have the same resonance excitation conditions (ingoing resonance), but different conditions for scattered light (outgoing resonance). Of the four possible backscattering configurations with circularly polarized light, only  $z(\sigma^+\sigma^-)\bar{z}$  exhibits double-resonance behavior. Note that another double resonance occurs in the  $z(\sigma^+, \sigma^-)\bar{z}$  configuration when the energy of incident photons is chosen to be at about  $\hbar\omega_L \approx 1.677$  eV, as expected from

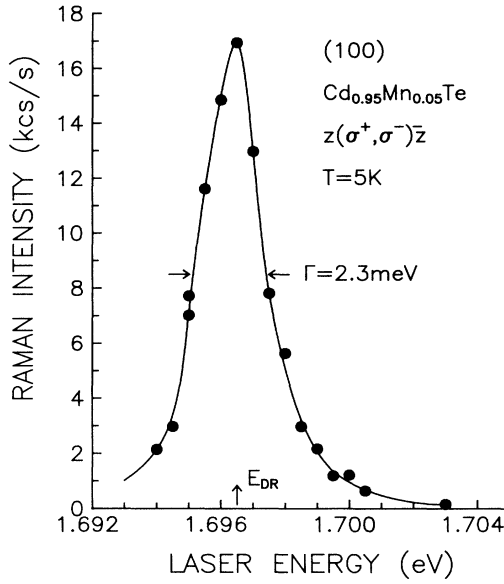


FIG. 4. Resonance profile of the Raman efficiency of the  $LO_1$  mode in  $Cd_{0.95}Mn_{0.05}Te$  in  $z(\sigma^+, \sigma^-)\bar{z}$  configuration. Double resonance occurs for an excitation energy  $E_{DR} = 1.6965$  eV at a magnetic field of  $H = 2.4$  T.

Fig. 1. Unfortunately, the intensity behavior of the  $LO$ -Raman peak could not be studied there due to the strong luminescence from the lowest exciton state. The double-resonance profile of the DRRS in the  $Cd_{1-x}Mn_xTe$  crystal is shown in Fig. 4. This profile was obtained by plotting the amplitude of the maximum of the magneto-Raman traces  $I_{RS}(H)$  (see Fig. 3) versus excitation energy  $E_L$ . The half-width of the resonance profile,  $\Gamma = 2.3$  meV, is nearly the same as the exciton half-width obtained from the reflectivity data.

## DISCUSSION

The DRRS just reported is connected with the large spin splitting of the electron states in SMS, particularly those that combine into the edge exciton states. Comparison of the excitation energies in double resonance with the exciton energies obtained from magnetorefectivity allows us to attribute the observed resonance to excitons associated with specific band-to-band transitions in the crystal.

The influence of exchange interaction on the exciton states in  $Cd_{1-x}Mn_xTe$  has been studied in a number of works.<sup>5,9,10</sup> Below we summarize the results.

Because of the large values of the fundamental gap  $E_g$  and the spin-orbit parameter  $\Delta_{so} \approx 1$  eV, the exchange interaction does not mix states from conduction, valence, and spin-orbit split bands, and all these bands can be treated independently. For a manganese mole fraction  $x = 0.05$  and magnetic fields  $H \leq 3$  T, typical for DRRS conditions in our samples, the exchange interaction is much larger than the Zeeman and cyclotron energies and the direct influence of the magnetic field on the electronic states can be neglected. Exchange interaction splits the

states in the  $\Gamma_6$  conduction band and  $\Gamma_8$  valence band. The  $\Gamma_6$  conduction band is split in two bands with spin  $|\frac{1}{2}\rangle_c$  and  $|\frac{1}{2}\rangle_c$ . The valence band  $\Gamma_8$  is split into four subbands with  $J = \frac{3}{2}$  and  $m_j = \frac{3}{2}, \frac{1}{2}, -\frac{1}{2},$  and  $-\frac{3}{2}$ . The energies of these states in mean-field approximation can be written as follows:<sup>9</sup>

$$\begin{aligned} E_c^1 &= E_g + 3A, & E_v^{1,4} &= \pm 3B, \\ E_c^2 &= E_g - 3A, & E_v^{2,3} &= \pm B, \end{aligned} \quad (1)$$

with  $A$  and  $B$  given by

$$A = \frac{1}{6}N_0x|J_e|\langle S \rangle_{H,T}, \quad B = \frac{1}{6}N_0x|J_h|\langle S \rangle_{H,T}, \quad (2)$$

where  $N_0$  is the number of the primitive cells per unit volume,  $x$  is the Mn mole fraction, and  $J_e$  and  $J_h$  are the constants responsible for the exchange interaction of the Mn ions with conduction- and valence-band electrons, respectively. For  $Cd_{1-x}Mn_xTe$  these constants are  $N_0J_e = 0.22$  eV,  $N_0J_h = -0.88$  eV.<sup>11</sup> Below we will take as a quantization axis the direction of the exchange field, i.e., the direction of the spin polarization of the Mn subsystem  $\langle S \rangle_{H,T}$ . Since the  $s$ - $d$  exchange interaction in SMS is ferromagnetic ( $J_e > 0$ ), the ground state of the conduction-band electron should be the  $S = \frac{1}{2}$  state. The  $p$ - $d$  exchange interaction with the valence-band electrons is antiferromagnetic ( $J_h < 0$ ) and thus the top valence band will be the  $m_j = \frac{3}{2}$  band. This notation is used in the schematic diagram of the transitions in Fig. 1.

The average spin polarization of the  $Mn^{2+}$  ions  $\langle S \rangle_{H,T}$  determines the dependence of the exchange interaction on magnetic field and temperature. It was found<sup>11</sup> that for  $H < 10$  T,  $\langle S \rangle_{H,T}$  in  $Cd_{1-x}Mn_xTe$  can be described by the modified Brillouin function  $B_S(t)$  with  $S = \frac{5}{2}$  as follows:

$$\langle S \rangle_{H,T} = S_0 B_S \left[ \frac{S\mu_B g_{Mn} H}{k_B(T + T_0)} \right], \quad (3)$$

$$B_S(t) = \frac{2S+1}{2S} \coth \left[ \frac{(2S+1)t}{2S} \right] - \frac{1}{2S} \coth \left[ \frac{t}{2S} \right], \quad (4)$$

where the empirical parameters  $S_0$  and  $T_0$  for  $Cd_{0.95}Mn_{0.05}Te$  are equal to  $S_0 = 2.11$  and  $T_0 = 0.29$  K.<sup>11</sup>

Variations of  $T$  and  $H$  change the average spin polarization  $\langle S \rangle_{H,T}$  and allow us to tune the spin splitting in order to adjust the electron bands to DRRS conditions. In cubic semimagnetic semiconductors, the exchange interaction is diagonal in the basis of the total momentum wave functions  $|J, m_j\rangle$  and does not mix the states with different  $m_j$ . The Coulomb interaction between electrons and holes leads to a formation of the exciton states downshifted with respect to the threshold interband transitions by the exciton binding energy  $E_R$ . For  $Cd_{1-x}Mn_xTe$  the difference in binding energy is very small for different exciton states and, neglecting effects of electron-hole exchange, the exciton spin splittings can be written as algebraic sums of valence- and conduction-band splittings. Only four exciton transitions are allowed in the Faraday configuration:

$$\begin{aligned}
E_{\text{ex}}^1 &= E_g - E_R + 3B + 3A, \\
E_{\text{ex}}^2 &= E_g - E_R + B - 3A, \\
E_{\text{ex}}^3 &= E_g - E_R - B + 3A, \\
E_{\text{ex}}^4 &= E_g - E_R - 3B - 3A.
\end{aligned}
\tag{5}$$

The first two transitions are allowed in  $\sigma^+$  polarization and the last two in  $\sigma^-$  polarization. DDRS occurs in our experiments when the laser energy coincides with  $E_{\text{ex}}^1$  and, simultaneously, the scattered photon energy coincides with  $E_{\text{ex}}^3$  as shown in the upper left corner of Fig. 1. The phonon-scattering process transfers an electron from the  $m_J = -\frac{3}{2}$  valence-band state to the  $m_J = \frac{1}{2}$  state. For DDRS the spin splitting between these states has to be equal to the phonon energy:

$$\Delta E = 4B = \frac{2}{3} N_0 x |J_h| \langle S \rangle_{H,T} = \hbar \Omega_{\text{LO}}. \tag{6}$$

Experimental results presented here have some interesting consequences for the microscopic mechanism of electron-phonon interaction responsible for DDRS in  $\text{Cd}_{1-x}\text{Mn}_x\text{Te}$ . Normally, deformation-potential interaction mediates transitions between different exciton states and would explain the experimental results discussed so far. However, this type of interaction cannot account for results from experiments performed on (110) surfaces of the same material. For these surfaces, backscattering by LO phonons is forbidden for both deformation-potential and intrinsic dipole-forbidden Fröhlich interaction.<sup>12</sup> In contrast to that, we have seen a  $\text{LO}_1$ -phonon line in the Raman spectrum of  $\text{Cd}_{1-x}\text{Mn}_x\text{Te}$  (110) with a strength and doubly resonant behavior roughly similar to that found for a (100) surface. An explanation of such

symmetry-forbidden Raman scattering may be connected with impurity-induced Fröhlich interaction scattering, which can be expected to be important in mixed crystals. Under resonance conditions, the elastic scattering by an impurity can cause an exciton transition from one exciton branch to another. Note that because of a large momentum transfer  $k$  involved in such a process this transition is not forbidden by symmetry since the valence-band states have a strongly mixed character for large  $k$  of an arbitrary direction. Impurity-induced Fröhlich interaction also can give a dominant contribution in symmetry-allowed scattering configurations due to its enhancement at larger wave vectors. A similar violation of Raman selection rules near resonance was reported recently for  $\text{Zn}_{1-x}\text{Mn}_x\text{Se}$  crystals,<sup>13</sup> where strong LO-phonon scattering was observed from a (110) surface even without magnetic field.

In summary, we have observed doubly resonant Raman scattering in the semimagnetic semiconductor  $\text{Cd}_{1-x}\text{Mn}_x\text{Te}$  by adjusting the exciton spin splitting, which is induced by strong exchange interaction with magnetic impurities. In Faraday configuration, DDRS appears only in crossed circular polarizations  $z(\sigma^+, \sigma^-)\bar{z}$  and is probably connected with disorder-enhanced phonon-induced electron transitions from  $|\frac{3}{2}\rangle_v$  to  $|\frac{1}{2}\rangle_v$  valence-band states.

#### ACKNOWLEDGMENTS

We are grateful for first-class technical assistance from H. Hirt, M. Siemers, and P. Wurster. S.I.G. acknowledges support from the Alexander von Humboldt Foundation.

\*Permanent address: Institute of Solid State Physics, 142432 Chernogolovka, Moscow district, USSR.

<sup>1</sup>F. Cerdeira, E. Anastassakis, W. Kauschke, and M. Cardona, *Phys. Rev. Lett.* **57**, 3209 (1986).

<sup>2</sup>T. Ruf, C. Trallero-Giner, R. T. Phillips, and M. Cardona, *Solid State Commun.* **72**, 67 (1989); *Phys. Rev. B* **41**, 3039 (1990).

<sup>3</sup>R. C. Miller, D. A. Kleinman, and A. C. Gossard, *Solid State Commun.* **60**, 213 (1986).

<sup>4</sup>F. Agulló-Rueda, E. E. Mendez, and J. M. Hong, *Phys. Rev. B* **38**, 12 720 (1980).

<sup>5</sup>J. K. Furdyna, *J. Appl. Phys.* **64**, R29 (1988).

<sup>6</sup>S. Venugopalan, A. Petrou, R. R. Galazka, A. K. Ramdas, and S. Rodriguez, *Phys. Rev. B* **25**, 2681 (1982).

<sup>7</sup>W. Limmer, S. Bauer, and W. Gebhardt, *J. Cryst. Growth* (to be published).

<sup>8</sup>To estimate  $x$ , we used an expression  $E_{\text{ex}} = (1.595 + 1.592x)$  eV after Y. R. Lee and A. K. Ramdas, *Solid State Commun.* **51**, 861 (1984).

<sup>9</sup>J. A. Gaj, J. Ginter, and R. R. Galazka, *Phys. Status Solidi B* **89**, 655 (1978).

<sup>10</sup>J. A. Gaj, in *Semiconductors and Semimetals*, edited by J. K. Furdyna and J. Kossut (Academic, San Diego, 1988), Vol. 25, p. 276.

<sup>11</sup>J. A. Gaj, R. Planel, and G. Fishman, *Solid State Commun.* **29**, 435 (1979).

<sup>12</sup>M. Cardona, in *Light Scattering in Solids II*, Vol. 50 of *Topics in Applied Physics*, edited by M. Cardona and G. Güntherodt (Springer-Verlag, Heidelberg, 1982), p. 18.

<sup>13</sup>W. Limmer, H. Leiderer, K. Jakob, W. Gebhardt, W. Kauschke, A. Cantarero, and C. Trallero-Giner, *Phys. Rev. B* **42**, 11 325 (1990).